New postcranial remains of large toxodontian notoungulates from the late Oligocene of Mendoza, Argentina and their systematic implications

SANTIAGO HERNÁNDEZ DEL PINO, FEDERICO D. SEOANE, and ESPERANZA CERDEÑO

During the last decade, the Deseadan (late Oligocene) Quebrada Fiera locality, Mendoza Province, Argentina, has provided a large amount of mammal remains. Taxonomic studies have shown the presence of faunal elements common with other Deseadan associations from Patagonia and lower latitudes (Salla, Bolivia), as well as endemic taxa of different groups of mammals (Notohippidae, Leontiniidae, Homalodotheriidae, Hegetotheriidae, and Metatheria) and even a gastropod. In this work, we present a taxonomic and phylogenetic analysis of a set of postcranial fossils of three families of the suborder Toxodontia (Notoungulata). The postcranial elements are assigned to taxa previously recognized at Quebrada Fiera, such as the leontiniid *Gualta cuyana* and the homalodotheriid *Asmodeus petrasnerus*, but also to the family Toxodontidae that is represented by *Proadinotherium* sp. and another larger toxodontid; a few dental remains of *Proadinotherium* are also included as this is the first time that toxodontids from Quebrada Fiera are described. In the case of *A. petrasnerus*, an almost complete calcaneum allows us to expand the diagnosis of this taxon. The bones assigned to *G. cuyana* enlarge the anatomical knowledge of this species. In turn, the presence of the genus *Proadinotherium* extends its geographic distribution in Argentina and adds to the extra-Patagonian record of *P. saltoni* from Salla, Bolivia. Phylogenetic results do not differ much from previous analyses using postcranial characters, and the obtained consensus trees show low node supports. The various phylogenetic analyses performed here provide a more robust framework to interpret the relationships of the studied taxa.

Key words: Mammalia, Toxodontidae, Leontiniidae, Homalodotheriidae, postcranium, Deseadan Age, Argentina, Mendoza.

Santiago Hernández Del Pino [stgo86@gmail.com] and Esperanza Cerdeño [espe@mendoza-conicet.gob.ar], Paleontología, Instituto de Nivología, Glaciología y Ciencias Ambientales, Centro Científico Tecnológico-CONICET-Mendoza. Avda, Ruiz Leal s/n, 5500 Mendoza, Argentina.
Federico D. Seoane [seoane.federico@gmail.com], Universidad de Buenos Aires, CONICET, Instituto de Estudios Andinos Don Pablo Groeber (IDEAN), Facultad de Ciencias Exactas y Naturales, Ricardo Güiraldes 2160, C1428EGA Buenos Aires, Argentina.

Introduction

Recent research on the Deseadan fauna (late Oligocene) from Quebrada Fiera, south of Mendoza Province, Argentina (Fig. 1), evidences a rich mammal assemblage that shows the existence of common elements with Deseadan faunal associations of Patagonia and those of lower latitudes such as Salla, Bolivia, as well as endemic taxa of different groups. Endemism refers to Notohippidae (*Mendozahippus fieriensis* Cerdeño and Vera, 2010), Leontiniidae (*Gualta cuyana* Cerdeño and Vera, 2015), Homalodotheriidae (*Asmodeus petrasnerus* Seoane and Cerdeño, 2014) and Metatheria (*Fieratherium sorex* Forasiepi, Goin, Abello, and Cerdeño, 2014); to these mammals a new terrestrial snail has been recently added (Miquel and Cerdeño 2016).

The fossiliferous site of Quebrada Fiera was discovered in the seventies during a geological prospection carried out by Yacimientos Petrolíferos Fiscales (YPF); its geological characterization and a preliminary faunal list were published by Gorroño et al. (1979). The stratigraphic section is composed of a heterogeneous conglomeratic level with variable matrix. The fossil-bearing beds consist of uniform sequences of tuffa-
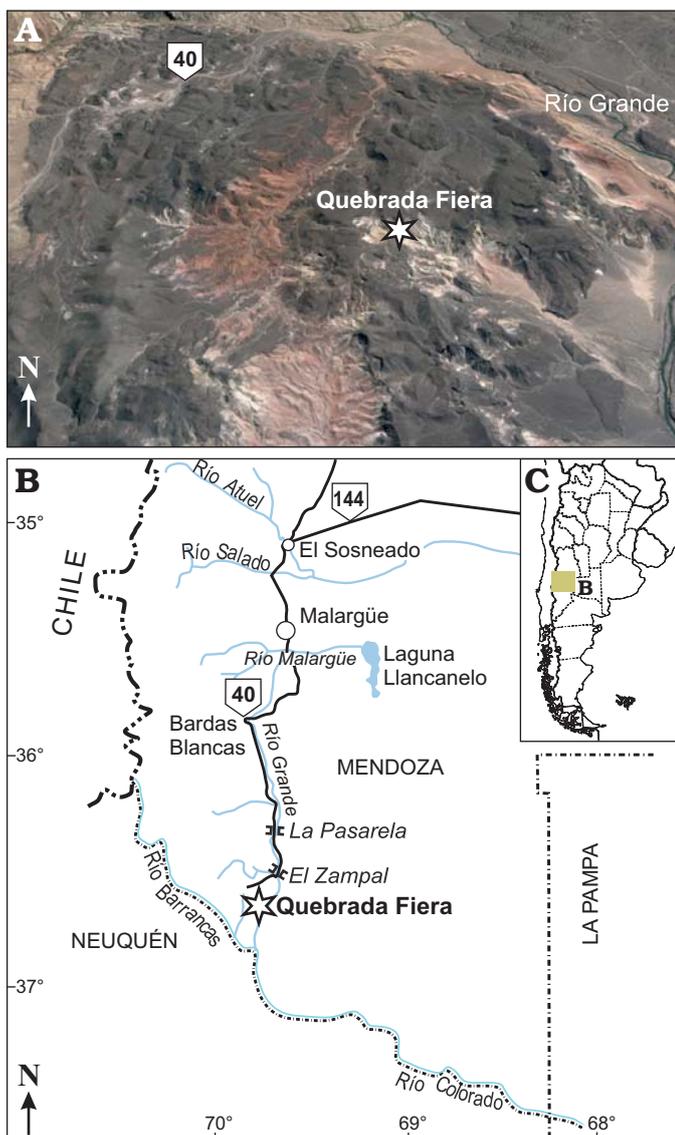
Acta Palaeontol. Pol. 62 (1): 195–210, 2017

https://doi.org/10.4202/app.00301.2016

Fig. 1. Google Earth view of Quebrada Fiera site (**A**). Location of the study area on the map of Argentina (**C**). Geographical location (asterisk) of the fossil locality (**B**). {fig. will be grayscale in printed version}

ceous paleosols intercalated with pyroclastic deposits, which are recognized as the base of the Agua de la Piedra Formation (Combina and Nullo 2011). Majority of fossils come from the northern side of the ravine, located at around 36°33'13.3'' S, 69°42'3.5'' W, 1300–1406 m altitude, but some have been also recovered from the southern side, at around 36°33'26'' S, 69°41'35'' W, 1316 m (see Cerdeño and Vera 2014).

Taxonomic studies of notoungulates based on postcranial characters are not common (e.g., Cifelli 1983; Shockey et al. 2012; Lorente et al. 2014) and they often provide imprecise assignations. Notoungulates are the most diverse group of the South American native ungulates and they display a great range of morphological disparity (Simpson 1936; Patterson and Pascual 1972; Bond 1986; Cifelli 1993; Croft 1999; Cassini et al. 2012). Traditionally, the suborder Toxodontia comprised five families (Isotemnidae, Homalodotheriidae, Leontiniidae, Notohippidae, and Toxodontidae), but in the past few years new phylogenetic analyses have questioned the monophyly of Isotemnidae and Notohippidae (e.g., Cifelli 1993; Shockey 1997; Cerdeño and Vera 2010; Billet 2011; Deraco and García López 2015). In this paper, we focus on the study of postcranial bones of three families (Homalodotheriidae, Leontiniidae and Toxodontidae); some of these bones were preliminarily identified as belonging to Toxodontidae (Hernández Del Pino et al. 2013), but now are interpreted differently. A few toxodontid dental remains from Quebrada Fiera are also included herein as this is the first description of this group for this locality.

Toxodontids were medium-to-large-sized herbivores, with euhypsodont, tusk-like incisors and protohypsodont to euhypsodont molars (Forasiepi et al. 2015). They are known from Oligocene to early Holocene in South America. Concerning late Oligocene, first described taxa were *Proadinotherium leptognathum* Ameghino, 1894, *Pronesodon cristatus* Ameghino, 1891, and *Pronesodon robustus* Ameghino, 1894 from localities in Chubut and Santa Cruz provinces in Patagonia. Later, Ameghino (1897, 1902) added new species of *Proadinotherium* and *Pronesodon* coming from Colhuehuapian levels (early Miocene) in Patagonia: *Proadinotherium angustidens* Ameghino, 1897, *Proadinotherium muensteri* Ameghino, 1902, and *Pronesodon vates* Ameghino, 1902. Synonymies at generic level were previously proposed (e.g., Simpson 1945), but all the species are in need of a thorough taxonomic revision to reach a confident conclusion. *Proadinotherium* Ameghino, 1894 has been also recorded from the Deseadan of Salla, Bolivia, with the species *P. saltoni* Shockey and Anaya, 2008. Following Madden (1990: 286), previous extra-Patagonian records of the genus would come from Tremembé (Brazil) and Chaparral (Colombia). The latter was tentatively identified by the author as *Proadinotherium* cf. *P. leptognathum*, without further comments. The Brazilian record, however, is not confirmed in later papers such as that by Berqvist and Ribeiro (1998).

The family Leontiniidae is known from Eocene to middle Miocene of South America (Bond and López 1995; Villarroel and Coldwell Danis 1997; Ribeiro and Bond 2000; Deraco et al. 2008; Shockey et al. 2012; Cerdeño and Vera 2015). Leontiniids reached their maximum taxonomic diversity during the Deseadan SALMA, with the presence of five genera in Patagonia, Argentina, and a total of seven in the South American continent (Shockey et al. 2012; Cerdeño and Vera 2015). They were large-sized herbivores with brachydont to mesodont dentition.

The rare, little diversified family Homalodotheriidae includes large mammals characterized, among other features, by a complete, closed brachydont dentition, the anteroproximal concave projection of the distal articulation of metacarpi and the cleaved third phalanges (Ameghino 1891; Elissamburu 2010; Cassini et al. 2012). The material from Quebrada Fiera was recognized as the new species *Asmodeus petrasnerus*, based on postcranial bones (Seoane and Cerdeño 2014). The holotype is a fragment of calca-

neum and the recent finding of a complete bone allows us to complete its characterization.

Institutional abbreviations.—AMNH, American Museum of Natural History, New York, USA; MACN, Museo Argentino de Ciencias Naturales "B. Rivadavia", Buenos Aires, Argentina; MCNAM, Museo de Ciencias Naturales y Antropológicas "J.C. Moyano", Mendoza, Argentina; MLP, Museo de La Plata, La Plata, Argentina; MNHN, Muséum national d'Histoire naturelle, Paris, France; MPM, Museo Regional Provincial Padre M. Jesús Molina, Río Gallegos, Argentina; YPM, Yale Peabody Museum of Natural History, New Haven, USA.

Other abbreviations.—APD, anteroposterior diameter; GC, group present/contradicted; MPTs, most parsimonious trees; PCR, positional congruence (reduced); SALMA, South American Land Mammal Age; TD, transversal diameter.

Material and methods

With the exception of three dental remains, the material from Quebrada Fiera herein studied consists of postcranial elements. The collection of Vertebrate Paleontology of the MCNAM, in Mendoza city, is the final repository for the studied material. Details of each specimen are included in the systematic section.

Taxonomic determination was done through morphologic and morphometric comparisons with different toxodontids (*Proadinotherium* Ameghino, 1894, *Adinotherium* Ameghino, 1887, *Pronesodon* Ameghino, 1894, and *Nesodon* Owen, 1853), leontiniids (*Gualta* Cerdeño and Vera, 2015, *Scarrittia* Simpson, 1934 and *Leontinia* Ameghino, 1894) and homalodotheriids (*Asmodeus* Ameghino 1894 and *Homalodotherium* Flower 1873). Majority of the material was directly observed at MLP and MACN by two of us (SHP and FS), and at AMNH and YPM by SHP; in addition, some photographs of leontiniids, homalodotheriids, and notohippids housed at AMNH were kindly provided by Barbara Vera and Andrea Elissamburu. Specimens belonging to the Ameghino collection in the MACN are referred to by the new inventory numbers, but their old equivalents are indicated in SOM 1, Supplementary Online Material available at http://app.pan.pl/SOM/app62-HernandezDelPino_etal_SOM.pdf, to facilitate comparisons with previous publications.

The large size of the material herein studied discards their belonging to the other toxodontian from Quebrada Fiera, the Notohippidae *Mendozahippus fierensis*, to which some postcranial bones have already been assigned (Cerdeño and Vera 2010, 2014). However, postcranial bones attributed to other notohippids are closer to some of the studied specimens and minor comparisons are included. In turn, mesotheriids (suborder Typotheria) are scarcely represented at Quebrada Fiera by *Trachytherus* cf. *T. spegazzinianus* Ameghino,

1889 (Cerdeño 2014); the general size of *Trachytherus* is smaller than most of the studied bones; just the calcaneum and astragalus assigned to toxodontids are roughly similar, but the morphology is different (see below and Shockey et al. 2007, 2016; Shockey and Anaya 2008).

All specimens revised directly or through original photographs are detailed in SOM 1.

For descriptions, we follow the protocol used by Cerdeño et al. (2012), considering six main faces for each element: proximal, distal, anterior (toward the head), posterior, medial (toward the sagittal plane), and lateral; besides, limb bones are considered in a vertical axis independently of the actual anatomical position. The terminology for the postcranium follows Cerdeño et al. (2012) and, when necessary, Constantinescu and Schaller (2012); for toxodontid dental anatomy, we follow Madden (1990) and Nasif et al. (2000).

The phylogenetic analysis is based on the character matrix from Shockey et al. (2012) modified by Cerdeño and Vera (2015), to which *Proadinotherium muensteri*, *Asmodeus osborni*, and the studied material from Quebrada Fiera (*Gualta cuyana* and *Asmodeus petrasnerus*) were added. Some character states were modified for nesodontine taxa. Character 2 (relative canine size) for *Adinotherium* and *Nesodon* was modified from state 1 (canine subequal in size to incisors, but none of the incisors are greatly enlarged) to state 2 (one of the incisors is caniniform and larger than any canine); character 5 (I2 enlarged caniniform), from 0 (absent) to 1 (present); character 25 (M1 mesiolingual cingulum), from 1 (present, extended only to protoloph) to 2 (absent); this character was originally codified with three states (Shockey et al. 2012), but there were only two values (0 and 1) in the matrix. Considering that toxodontids and notohippids do not present a well-developed cingulum in their molars and that homologies of the cingula with other structures are not clear for these two groups, we modified character 26, which referred to the posterior cingulum in upper molars, as "posterior fossette of upper molar" with two different states 0 (absent) and 1 (present) (see SOM 2).

A traditional search for maximum parsimony trees, on a matrix of 26 taxa and 81 characters, using TNT 1.5 program (Goloboff et al. 2008), was performed under different parameters. First, we conducted a search using characters equally weighted under 500 replicates, ten trees saved per replica and followed by a branch swapping with the trees retained; then we calculated the strict consensus tree from the resulting MPTs and a reduced consensus. To obtain the reduced consensus we used iterative PCR, a methodology proposed by Pol and Scapa (2009), which searches for unstable taxa or branches within the different tree topologies; it also detects which characters are conflictive and the missing entries responsible for alternative positions of the taxa or branches. The result is a tree with the unstable branches pruned, showing the alternative positions of unstable taxa.

A third analysis was performed using the extended implied weighting variant (Goloboff 2014) implemented in TNT, with different values of k (concavity constant), using

Mirande (2009) and Mirande et al.'s (2013) scripts. Unlike implied weighting, the extended implied weighting version prevents the assignation of artificially high weights to characters with many missing entries (Mirande et al. 2013).

For the strict consensus trees resulting from the analyses under equal weights, we calculated the GC "jack-knife" node support values under 1000 replicates; for the consensus trees obtained under implied weights, we calculated GC "symmetric resampling" node support values under 1000 replicates. Synapomorphies were mapped in the consensus trees using WinClada (Nixon 2002).

Systematic palaeontology

Notoungulata Roth, 1903

Toxodontia Owen, 1853

Toxodontidae Owen, 1845

Genus *Proadinotherium* Ameghino, 1894

Type species: *Proadinotherium leptognathum* Ameghino, 1894, La Flecha?, Santa Cruz Province, Argentina, Deseadan SALMA, late Oligocene.

Proadinotherium sp.

Fig. 2A–D, G.

Material.—MCNAM-PV 4238, right M2; MCNAM-PV 4960, left m2; MCNAM-PV 3843, left m3; MCNAM-PV 4085, right calcaneum; MCNAM-PV 4215, right astragalus. All from Quebrada Fiera, Mendoza, Argentina, Deseadan SALMA, late Oligocene.

Description.—Dentition: MCNAM-PV 4238 (Fig. 2A), an incomplete, worn right M2, is the only upper tooth from Quebrada Fiera so far assigned to Toxodontidae. It is similar in outline and appearance to the molars of *Adinotherium* (early Miocene, Santacrucian SALMA). Lingual and posterior borders as well as the roots are missing. The oclusal surface presents the typical Y-shaped central fossette, as well as two fossettes at the distal half; the most labially placed is circular and tiny whereas the other is larger and ovoid (length twice width), anterolabially–distolingually oriented; the ectoloph bears a wide, smooth paracone fold.

The m2 (MCNAM-PV 4960; Fig. $2B_1$, B_2) and m3 (MCNAM-PV 3843; Fig. $2C_1$–C_3) are narrow and high teeth. The trigonid is broken in m2, but appears to be almost quadrangular. In m3 the trigonid is crescent-shaped with the protoconid pointing anterolabially (as in m2). The m2 presents a fossettid formed by the closing of meta-entoconid fold and the accessory fossettid is not observable; instead, the m3 has the lingual folds open and a well-developed accessory fossettid. The morphology (quadrangular trigonid, closed lingual folds and developed roots), size and degree of wear of the m2 correspond to an adult specimen whereas the very little worn m3 resembles the recently erupted molars of young specimens of *Adinotherium* (e.g., AMNH 9517; see also Scott 1912: pl. 18).

Table 1. Comparative dimensions (in mm) of the calcanei from Quebrada Fiera, Mendoza. [1] from photographs of specimens taken by SHP and FS; [2] after Cerdeño and Vera (2015); [3] completed after Seoane and Cerdeño (2014). Values in parentheses are approximate. APD, anteroposterior diameter; H, height; TD, transversal diameter; – measurement not available.

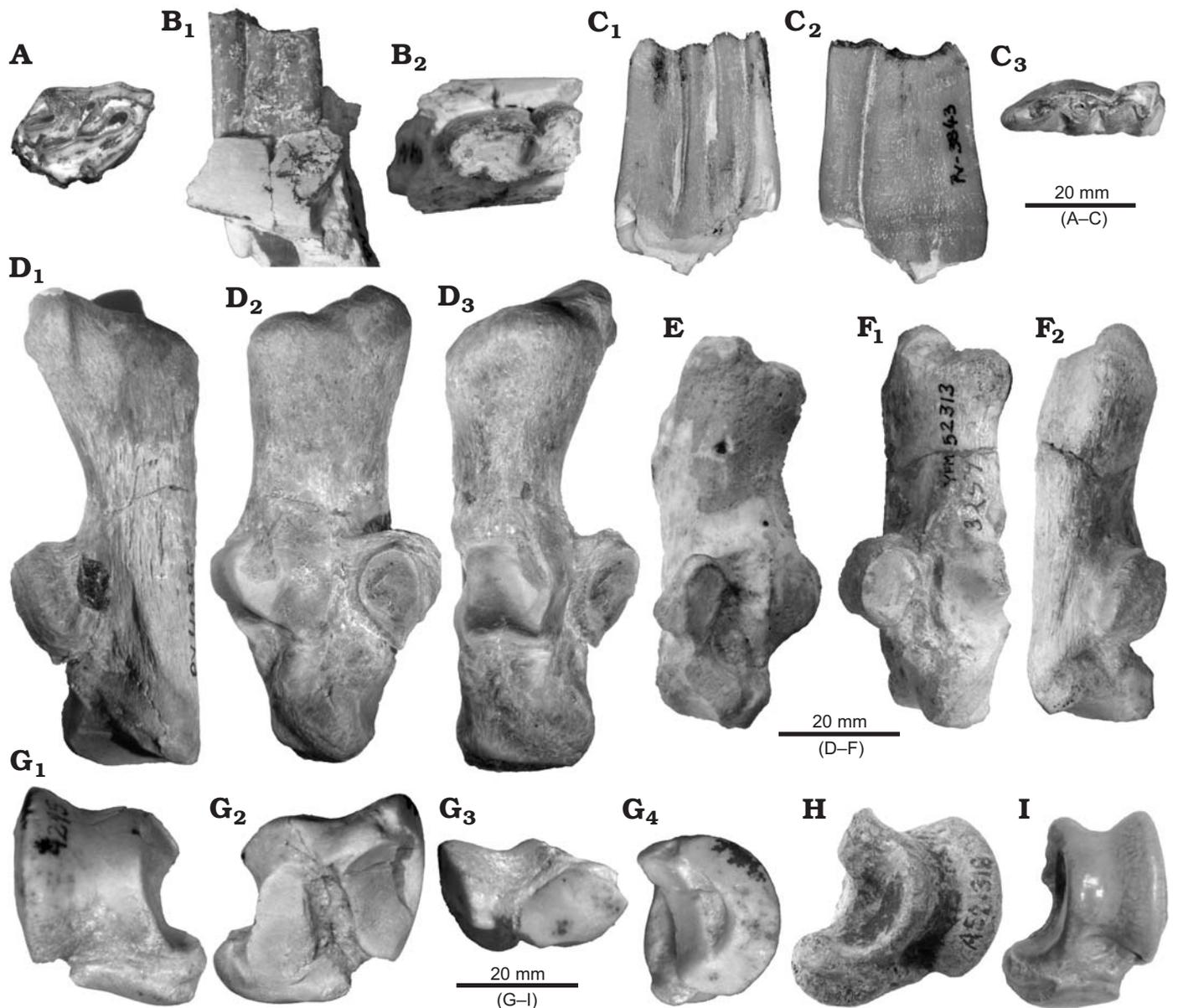|	H	Tuber		Sustentaculum (calcaneum) TD	Maximal APD (at fibular facet level)	Distal articulation		Maximum distal TD	Minimum posterior TD
		TD	APD			TD	APD		
Proadinotherium sp. MCNAM-PV 4085	80.8	27.6	28.7	29.7	35.0	20.5	16.3	22.6	17.8
Toxodontidae gen. et sp. indet. MCNAM-PV 3907	–	40.2	35.4	–	–	–	–	–	(22.1)
Proadinotherium muensteri[1] MACN Pv-17576	67.1	28.3	29.8	26.2	27.1	18.4	23.7	24.3	15.8
Adinotherium sp.[1] MACN A 2100	52.0	–	18.3	–	(23.2)	11.8	–	–	–
MACN A 1016	56.8	–	23.3	–	(26.6)	10.6	–	–	–
MACN A 1020	51.1	–	19.6	–	(23.5)	(15.1)	–	–	–
MACN A 8515	58.5	21.6	(25.4)	(18.7)	–	–	–	16.6	15.3
Gualta cuyana MCNAM-PV 3916[2]	97.1	42.0	44.8	> 43	53.5	–	–	–	31.5
MCNAM-PV 4283[2]	102.2	43.0	(48.9)	(49.5)	55.8	39	30.2	39	–
MCNAM-PV 4412	–	47.2	44.1	–	–	–	–	–	–
Scarrittia[3] AMNH 29585	138.6	52.6	63.0	73.4	(70)	–	–	46.0	(37)
Asmodeus petrasnerus MCNAM-PV 4958	170.8	69.0	76.1	> 53	74.9	30.3	39.7	(58.5)	26.2
MCNAM-PV 5077	–	–	–	–	(72)	–	–	(52)	(30.5)
MCNAM-PV 4101[3]	–	–	–	–	68.0	30.0	34.0	45.5	–
MCNAM-PV 3906[3]	–	–	–	–	71.0	> 29	36.0	(44.6)	–
Asmodeus osborni[1] MACN 12327	280.0	111	128	127	101	31.0	49.5	69.6	45.6

Fig. 2. Toxodontian notoungulates from South America. **A–D**. *Proadinotherium* sp. from Quebrada Fiera, Mendoza, Argentina; Deseadan SALMA (late Oligocene). **A**. MCNAM-PV 4238, right M2, occlusal view. **B**. MCNAM-PV 4960, left m2, labial (B_1) and occlusal (B_2) views. **C**. MCNAM-PV 3843, left m3, lingual (C_1), labial (C_2), and occlusal (C_3) views. **D**. MCNAM-PV 4085, right calcaneum, posterior (D_1), medial (D_2), and anterior (D_3) views. **E**. *Proadinotherium muensteri* Ameghino, 1902 from Colhue Huapi lake, Chubut, Argentina; Colhuehuapian SALMA (early Miocene), MACN Pv-17576 (cast), left calcaneum, medial view. **F**. *Rynchippus equinus* Ameghino, 1897 (Notohippidae) from Salla, Bolivia; Deseadan SALMA (late Oligocene), YPM VP-52313, left calcaneum, anterior (F_1) and posterior (F_2) views. **G**. *Proadinotherium* sp. from Quebrada Fiera, Mendoza, Argentina; Deseadan SALMA (late Oligocene), MCNAM-PV 4215, right astragalus, anterior (G_1), posterior (G_2), distal (G_3), and lateral (G_4) views. **H**. *Proadinotherium leptognathum* Ameghino, 1894 from Santa Cruz, Argentina; Deseadan SALMA (late Oligocene), MACN A 12319, left astragalus, anterior view. **I**. "*Morphippus imbricatus*" Ameghino, 1897 (Notohippidae) from Sarmiento Formation, Chubut, Argentina; Deseadan SALMA (late Oligocene), MACN A 12100, left astragalus, anterior view.

Calcaneum: MCNAM-PV 4085 (Fig. 2D; Table 1) is a relatively small and gracile bone, more elongated and with more slender body than the calcanei of *Nesodon* and *Adinotherium*. Its size is slightly greater than that of *Proadinotherium muensteri* (e.g., MACN Pv-17576; Fig. 2E, Table 1), *Proadinotherium* sp. (e.g., YPM VP-25075) and *Adinotherium* (e.g., MACN 2100, MACN 8515; Table 1), but they share the general outline and disposition of the articular

facets. The tuber is relatively short (APD) and wide, with its posteromedial area projecting both medially and proximally. There is a well-marked posteromedial depression on the tuber corresponding to the tendinous sulcus (Fig. 2D$_1$), which does not extend on the proximal face. The sustentaculum is short and the sustentacular facet is subelliptic and flat, placed at a rather vertical plane (Fig. 2D$_3$). The ectal facet is high and narrow, subdivided into two main flattened

areas that make a smooth angle in between, which results in a slight convexity of the whole articulation, medially oriented. The fibular facet is very convex, barely projected proximally and distally; although it projects anteriorly from the corpus of the bone, difference with the anterior point of the tuber is not great, which render a roughly rectangular outline to the calcaneum in lateral view. The contact between the fibular and ectal facets is at the distal part of the latter (Fig. 2D$_2$, D$_3$). In anterior view, the distal area of the bone is wide, hiding the navicular facet on the medial face. The latter is seen in medial view; it is elliptical and placed at the distal border; it reaches the sustentacular facet and forms an angle of ~60°. The distal facet for the cuboid is concave and kidney-shaped and differs from *P. muensteri*, whose facet is less concave and more squared.

Astragalus: The morphology and size of MCNAM-PV 4215 (Fig. 2G, Table 2) are similar to those of *Proadinotherium muensteri* (MACN A 12048; Fig. 2H) and *Adinotherium* (Scott 1912). The bone is relatively higher and narrower than specimens assigned to or labeled as *Pronesodon* and *Nesodon* (Ameghino 1894; Scott 1912; SHP personal observation). The trochlea is asymmetrical and deeper than in these two genera; the lateral condyle is much more developed than the medial one (Fig. 2G$_1$). On the posterior face, there are two articular facets for the calcaneum, higher than wide (height double width), separated by a deep, wide groove (Fig. 2G$_2$). The lateral facet is proximodistally concave and a long depression separates it from the lateral side of the trochlea. The medial facet is flattened, wider distally than proximally; it reaches the posterior part of the navicular facet. At the proximal end of the groove between facets, there is a tiny astragalar foramen that does not go through the bone. The astragalar neck is short, but more developed than in *Pronesodon* and *Nesodon*. The navicular articulation (Fig. 2G$_3$) is very convex anteroposteriorly, but wide and extended medially with respect to the trochlea; its APD is greater laterally than medially. On the medial face, the trochlea presents two projected articular areas; the proximal one is small and subtriangular whereas the other extends mediodistally forming like a shelf supported by a tuberosity placed over the

lateral end of the navicular facet. Both areas take part in the articulation with the tibia and are barely united to each other by the trochlear border. On the lateral face (Fig. 2G$_4$), the depression posterior to the trochlear border is elongate, with its proximal end reaching the narrow separation between the lateral side of the condyle and the calcaneum facet, such as occurs in the mentioned MACN A 12048.

As commented above, these two tarsals have a roughly similar size to the mesotheriid *Trachytherus*. For instance, the astragalus (Table 2) is relatively close to the smaller specimens of *T. alloxus* represented in the bivariate plot in Shockey et al. (2016: fig. 5A), but its morphology differs; the mesotheriid shows developed neck, semispherical distal facet, and a distolateral projection (see also Shockey et al. 2007). The calcaneum (Table 1) is clearly longer than that of *T. alloxus* (Shockey and Anaya 2008: 153 and appendix), which differs in the tuber, without proximomedial projection, and the relative position of astragalar facets, the sustentacular one, more distally placed (Shockey and Anaya 2008: fig. 7.8).

With respect to notohippids, the tendinous sulcus of the calcaneum is deeper in this group; AMNH 29579 (listed as *Rhynchippus pumilus* by Shockey et al. 2012: appendix 2) and YPM VP-52313 (labeled as *R. equinus*) are much smaller and with the tuber less projected posteromedially (Fig. 2F). The astragalus MACN A 12100, labeled as "*Morphippus imbricatus*" Ameghino, 1897 (Fig. 2I), is relatively narrower than MCNAM-PV 4215, its medial condyle is higher, which render the trochlea deeper, and the neck is relatively longer; besides, the lateral condyle is less acute, the sustentacular facet is narrow distally (contrary to that of MCNAM-PV 4215), and the proximomedial corner is less projected.

Toxodontidae gen. et sp. indet.

Fig. 3.

Material.—MCNAM-PV 3907, left calcaneum fragment from Quebrada Fiera, Mendoza, Argentina, Deseadan SALMA, late Oligocene.

Description.—The specimen MCNAM-PV 3907 (Fig. 3, Table 1) consists of the tuber and a fragment of the ectal facet

Table 2. Comparative measurements (in mm) of the astragali of *Proadinotherium* sp. and *Gualta cuyana* from Quebrada Fiera, Mendoza. [1] photographs of *Scarrittia* taken by Barbara Vera and Andrea Elissamburu. Values in parentheses are approximate. APD, anteroposterior diameter; H, height; TD, transversal diameter; – measurement not available.

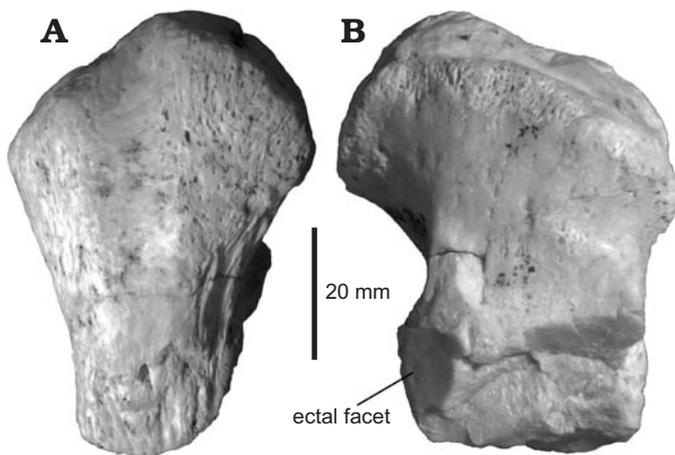|	Maximum		Trochlea		Distal		Medial APD
	TD	H	TD	H	TD	APD	
Proadinotherium sp. MCNAM-PV 4215	26.5	28.9	16.6	25.5	20.3	13.5	18.0
Proadinotherium muensteri MACN A 12048	26.5	28.0	20.0	25.0	21.0	19.5	20.5
Gualta cuyana MCNAM-PV 4089	(46.5)	(48.8)	30.9	46.7	> 31	26.2	35.0
MCNAM-PV 4303	58.0	50.0	33.5	45.5	42.0	28.4	34.4
MCNAM-PV 4891	56.6	47.0	37.9	42.3	40.5	28.0	32.5
MCNAM-PV 4896	–	–	38.6	(46.5)	–	–	32.2
Scarrittia[1] AMNH 29585	84.5	75.5	59.0	70.5	–	–	48.0

Fig. 3. Toxodontidae gen. et sp. indet. from Quebrada Fiera, Mendoza, Argentina; Deseadan SALMA (late Oligocene), MCNAM-PV 3907, left calcaneum fragment, posterior (**A**) and anterior (**B**) views.

of a calcaneum that is larger and more robust than that assigned to *Proadinotherium* (Fig. 2D). The tuber is short in APD and wider, more rectangular outlined than in MCNAM-PV 4085. The medial half of the tuber is elevated, but less pointed. The tendinous sulcus is relatively longer and more centered on the posterior face (Fig. 3A). The remaining facet indicates that the "neck" of the bone (Fig. 3B) is shorter than in MCNAM-PV 4085. Compared with the calcanei of the leontiniid *Gualta cuyana* (Cerdeño and Vera 2015), MCNAM-PV 3907 is a little smaller, the tuber is relatively wider and presents a well-developed tendinous sulcus that is hardly marked in the specimens of *Gualta*; besides, though the area is incomplete, it seems that the medial and the sustentacular facets for the astragalus would be closer than in the leontiniid. Therefore, we assign tentatively the calcaneum fragment MCNAM-PV 3907 to a toxodontid; based on its size and differences with *Proadinotherium*, it could correspond to a taxon more similar to the lower Miocene genus *Nesodon*, which could be the genus *Pronesodon* if the deep revision of this taxon eventually confirms its taxonomic validity. With respect to *Nesodon* (e.g., MACN A 9070–9073), MCNAM-PV 3907 has a better

marked tendinous sulcus, the tuber is not anteriorly pointed (lower APD) and the neck is relatively shorter. These features might imply not only taxonomic but functional differences, but this evaluation is beyond the aim of this paper.

Leontiniidae Ameghino, 1894
Genus *Gualta* Cerdeño and Vera, 2015

Type species: *Gualta cuyana* Cerdeño and Vera, 2015, Quebrada Fiera, Mendoza Province, Argentina, Deseadan SALMA, late Oligocene.

Gualta cuyana Cerdeño and Vera, 2015
Figs. 4–6.

Material.—MCNAM-PV 4696, associated left pyramidal, magnum, unciform, and fragment of Mc III; MCNAM-PV 5078, associated left pyramidal, unciform and fragments of humerus and ulna; MCNAM-PV 4094, MCNAM-PV 4785, incomplete tibiae; MCNAM-PV 4303, MCNAM-PV 4891, MCNAM-PV 4089, two right and one left astragali; MCNAM-PV 4894, MCNAM-PV 4896, right and left astragalus fragments; MCNAM-PV 4412, calcaneum fragment; MCNAM-PV 5035, left navicular. All material from Quebrada Fiera, Mendoza Province, Argentina, Deseadan SALMA, late Oligocene.

Description.—Forelimb: The specimen MCNAM-PV 4696 (Fig. 4A–F, Table 3) includes the pyramidal, magnum, unciform and part of the Mc III of a same individual. The pyramidal (Fig. 4A$_1$–A$_4$) is a low, irregular bone. The anterior face is convex and projected laterodistally; the lateral face is wrinkled and presents a proximolateral prominence; below and posterior to it there is a high semicircular facet for the pisiform. The proximal facet is large, almost occupying the whole face; its APD is greater than the TD; it is transversely concave and the medial border is straight (Fig. 4A$_3$). This border forms a crest with the medial facet, which is long in APD and low: it is flattened, but with a slight crest in the middle that barely differentiates two articular areas. Below this facet, there is a shallow, wrinkled depression. On the distal face (Fig. 4A$_4$), there is a big subtriangular facet for the unciform (Fig. 4F); it is anteriorly wide and transversely

Table 3. Measurements (in mm) of the carpals and metacarpal of *Gualta cuyana* from Quebrada Fiera, Mendoza. Values in parentheses are approximate. APD, anteroposterior diameter; H, height; TD, transversal diameter.

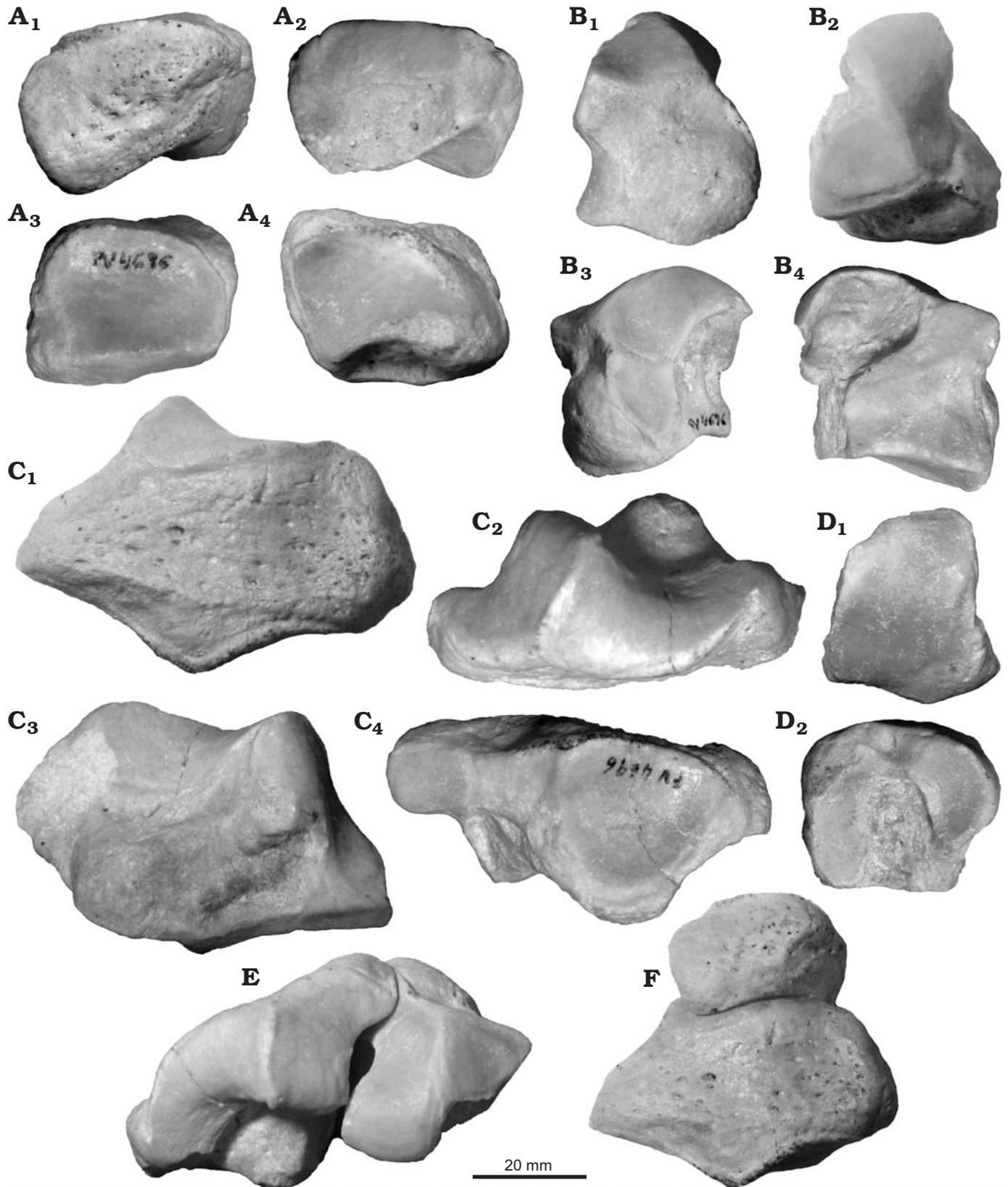| Pyramidal	Maximum			Proximal facet		Distal facet	
	TD	APD	H	TD	APD	TD	APD
MCNAM-PV 4696	24.8	32.1	23.3	18.7	27.1	17.8	24.1
MCNAM-PV 5078	23.3	30.1	20.3	17.2	25.5	17.9	23.0
Magnum	Anterior TD	Proximal tuberosity TD	Maximum H	Anterior H		Distal TD	
MCNAM-PV 4696	31.6	17.4	(35)	28.1		29.0	
Unciform	Maximum			Posterior H		Posterodistal facet	
	TD	APD	H			TD	APD
MCNAM-PV 4696	29.5	58.4	42.3	29.0		26.2	27.8
MCNAM-PV 5078	27.0	52.5	40.1	26.2		25.4	25.6
Metacarpal III	Proximal epiphysis			Proximal facet			
	TD		APD	TD		APD	
MCNAM-PV 4696	34.6		38.1	29.1		38.1	

Fig. 4. Left carpals and metacarpal of leontiniid notoungulate *Gualta cuyana* Cerdeño and Vera, 2015 from Quebrada Fiera, Mendoza, Argentina; Deseadan SALMA (late Oligocene), MCNAM-PV 4696. **A**. Pyramidal, anterolateral (A_1), medial (A_2), proximal (A_3), and distal (A_4) views. **B**. Magnum, anterior (B_1), proximal (B_2), lateral (B_3), and medial (B_4) views. **C**. Unciform, anterolateral (C_1), proximal (C_2), medial (C_3), and distal (C_4) views. **D**. Proximal fragment of McIII, proximal (D_1) and lateral (D_2) views. **E**. Magnum and unciform in anatomical position, proximal view. **F**. Pyramidal and unciform in anatomical position, anterolateral view.

concave, and narrows posteriorly, becoming convex and reaching the lateroposterior facet for the pisiform.

The magnum (Fig. 4B) shows a trapezoidal anterior face, with a notch on the medial border; a strong rounded tuberosity occupies most part of the face, surrounded by a shallow proximomedial depression (Fig. 4B$_1$). The proximal face (Fig. 4B$_2$) bears two facets that rise posteriorly with a crest in between. The medial one articulates with the scaphoid; it is subtriangular, as wide as long (APD), and projects medially in anterior view. The other proximal facet is for the semilunate; it elevates backward over a protuberance of the bone, becoming very convex, whereas the most anterior area directs laterally and contacts the lateral facet for the unciform. Just behind the limit of the proximal facet, the bone is low, but the posterior apophysis is lacking. The unciform facet is subcircular-trapezoidal and reaches the distal border (Fig. 4B$_3$). Behind this facet and below the proximal border, there is a wrinkled concavity. On the medial face of the bone, forming an angle greater than 90° with the proximal facet, there is a flat, quadrangular articulation for the trapezoid, projected backwards in a narrow edge, and well separated from the distal border by a concave, wide area where the Mc II would fit (Fig. 4B$_4$). Behind the border of the superior medial facet, the bone has another wrinkled depression. Distally there is a smoothly concave facet, anteriorly wide and tapering backwards.

The unciform (Fig. 4C) is long and low. The proximal face is formed by two large facets placed at a strong angle and forming a distinctive acute crest (Fig. 4C$_1$, C$_2$). The most anterior facet, for the semilunate, is smoothly concave-convex, high and narrow, steeply inclined anterodistally and protruding medially at its proximomedial area. The facet for the pyramidal is very concave anteroposteriorly, but transversely convex at its anterior half, where it projects laterally whereas the distal half inclines medially. The posterior limit of this facet is a posterior, narrow and convex tuberosity, whose most proximal area is smooth and could fit with the pisiform, even though there is not a well-defined facet. The lateral face of the bone is flattened, with the central portion a little depressed; its distal border approximates a very open "V" in contrast to the proximal inverted "V" (due to the crest between the two proximal facets) (Fig. 4C$_2$). On the medial face, below the projection of the proximal facet, there is a strong, low tuberosity that widens the bone at this level (Fig. 4C$_3$). In distal view, there is a great concave subtriangular facet for the Mc IV. It forms a marked angle (~50º) with a second articular surface differentiated into two flat zones, for the articulation with the lateral and proximolateral facets of the magnum; therefore, anatomically, these two facets are medial and not distal, but are distally oriented (Fig. 4C$_4$, 4E).

The fragment of the Mc III (Fig. 4D$_1$, D$_2$) has a large, trapezoidal proximal facet that fits with the described magnum; it is deeper (APD) than wide. On the medial face, there are two small facets for the Mc II, the anterior one more developed in height. Laterally, there are two large, high and slightly concave facets for the Mc IV; the posterior one is

more proximally placed whereas the anterior one is a little separated from the proximal border; both facets are separated by a shallow depression, although there is a short bony "bridge" between them at the proximal area.

A second set of associated bones (MCNAM-PV 5078) is composed of the left pyramidal and unciform highly comparable to those herein described and just slightly smaller (Table 3); together with them there are small portions of the ulna and humerus, which are too incomplete to make comparisons; only the humerus trochlea reveals a smaller size than the specimens MCNAM-PV 3938 and MCNAM-PV 4376 previously described for *Gualta cuyana* (Cerdeño and Vera 2015).

Based on the short descriptions of these bones for the leontiniid *Scarrittia* (Chaffee 1952) and the toxodontid *Nesodon* (Scott 1912), it is not easy to establish clear morphological differences between the two groups. As a whole, our material seems to be very close to *Scarrittia* when compared with the forefoot AMNH 29582, although some differences exist. Some features of our pyramidal (proximal facet not ovoid, having a straight medial border, and lacking an anteromedial tubercle) separate it from *Nesodon* (Scott 1912). The unciform differs from both compared taxa in the absence of a well-developed facet for Mc V; the subtriangular distal facet for Mc IV differs from the quadrate outline described for *Nesodon*. The concavity of the anterior medial border of the magnum also differs from both taxa, in which this border is straighter. The angle of the anterolateral border of the unciform is less acute than that of both genera, based on the figure of *Nesodon* (Scott 1912: pls. 22, 5) and the photographs of AMNH 29582 of *Scarrittia*. The width of the proximal epiphysis and the angle between the two proximal facets of Mc III are closer to that observed in *Scarrittia*. Despite the particularities of the described postcranial bones, it seems confident to refer them to the leontiniid *Gualta cuyana* instead to the toxodontids recognized at Quebrada Fiera.

As stated in the introductory paragraphs, the studied bones are discarded to belong to the notohippid *Mendozahippus fierensis* (Cerdeño and Vera 2010, 2014). Even though preserved fragments are not homologous, the proximal TD of the Mc III assigned to *G. cuyana* measures 34.6 mm (Table 3) whereas that of the Mt III of *Mendozahippus fierensis* is clearly smaller (12.4 mm; Cerdeño and Vera 2010: table 3). Measurements provided by Shockey (1997: table 3) for *Eurygenium pacegnum* from Salla reflect that pyramidal and unciform are smaller than our specimens. With respect to mesotheriids, the morphology of the magnum and unci-

Table 4. Measurements (in mm) of the tibial fragments of *Gualta cuyana* from Quebrada Fiera, Mendoza. APD, anteroposterior diameter; TD, transversal diameter.

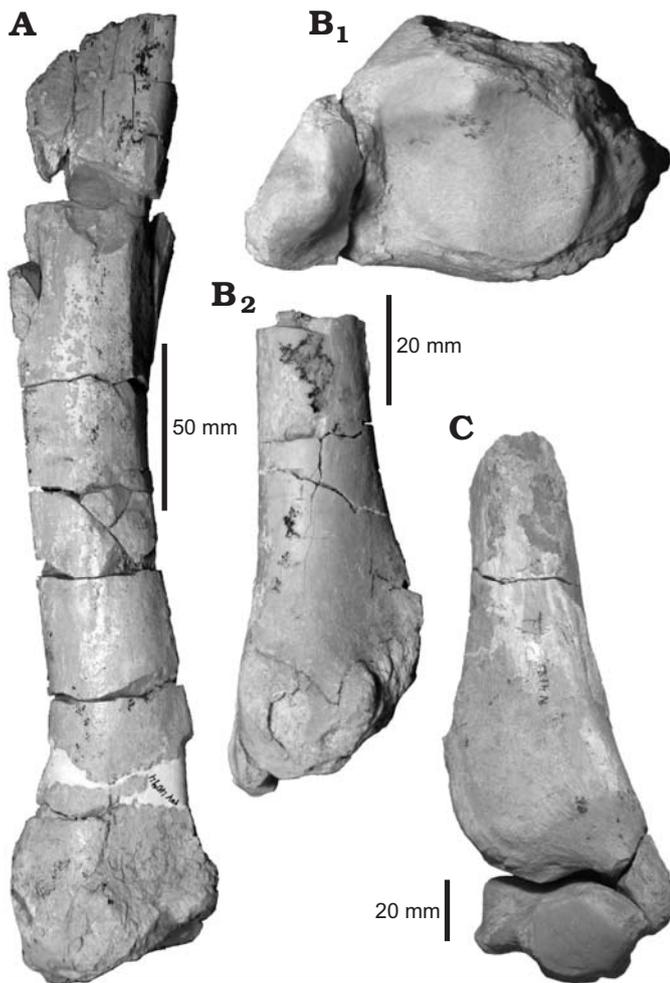|	Diaphysis		Distal epiphysis		Trochlear facet	
	TD	APD	TD	APD	TD	APD
MCNAM-PV 4094	32.1	31.0	70.4	(44.3)	(42.5)	35.3
MCNAM-PV 4785	36.4	33.4	68.3	52.1	41.0	34.4

Fig. 5. Tibiae of leontiniid notoungulate *Gualta cuyana* Cerdeño and Vera, 2015 from Quebrada Fiera, Mendoza, Argentina; Deseadan SALMA (late Oligocene). **A**. MCNAM-PV 4094, posterior view. **B**. MCNAM-PV 4785, distal (B₁) and posterior (B₂) views. **C**. Tibia, MCNAM-PV 4785, in anterior view and astragalus, MCNAM-PV 4891, in distal view.

form, for instance, is too different to consider their belonging to this group (Cerdeño et al. 2012; Shockey et al. 2016).

Hind limb.—The correspondence of some tibial fragments with the astragali assigned to leontiniids (see below) allows identification of the specimens MCNAM-PV 4094 and MCNAM-PV 4785 as *G. cuyana*. These specimens (Fig. 5A–C, Table 4) reveal that the tibia is relatively long and slender. The shaft is compressed laterally, trihedral in cross-section, becoming wider and more rounded toward the distal end (MCNAM-PV 4094; Fig. 5A). The tibial crest appears to be short, but it is incomplete. The distal epiphysis is rectangular in cross section, with a prominent medial malleolus that

bears a facet at the laterodistal end. The lateral side of the astragalar facet is more oblique and shallower than the medial one; both subfacets are separated by a low intercondylar ridge. Chaffee (1952) described the tibia of *Scarrittia* as a massive bone, which is not the case for MCNAM-PV 4094 (the most complete of the studied specimens). This difference cannot be adequately evaluated with the present sample, and a broader study of different long bones collected at Quebrada Fiera will be achieved soon. The studied tibiae are similar in outline to that of the toxodontid *Nesodon* (field number RB2-SHP-13-1, pending catalogue number at MPM-PV, SHP personal data), but with a distal epiphysis less quadrangular and a less vertical malleolus.

MCNAM-PV 4412 (Table 1) is a calcaneum fragment comparable to the specimens previously ascribed to *Gualta cuyana* (Cerdeño and Vera 2015). It preserves the tuber and the fibular and astragalar facets; the sustentaculum and the distal area are lacking.

Two of the referred astragali (MCNAM-PV 4891 and MCNAM-PV 4303) are very well preserved (Fig. 6A, Table 2). The bone is quadrangular in outline, much larger and robust than MCNAM-PV 4215 assigned to *Proadinotherium* (Fig. 2G). The trochlea is rather symmetrical and shallow (Fig. 6A₁, A₃); the distal articulation is little detached, with the astragalar neck reduced to a shallow groove. The medial condyle of the trochlea is more projected proximally in MCNAM-PV 4303 than in MCNAM-PV 4891. On the posterior face (Fig. 6A₂), there are two flattened facets for the calcaneum, the lateral one slightly concave. Both facets face posteriorly at a different plane and are separated by a deep groove that opens proximally, without forming an astragalar foramen, and widens distally toward the astragalar neck. The lateral facet is longer than the medial one, and it occupies the whole length of the posterior face, being wider proximally than distally, with a medial notch. The medial facet is more rounded and contacts distally with the navicular facet. The medial face of the bone shows a large articulation for the tibia expanded distomedially over the astragalar head. The latter is mostly occupied by the navicular facet that, however, does not reach the medial border. This articulation is subtrapezoidal, anteroposteriorly convex and rather straight transversely (Fig. 6A₃), although MCNAM-PV 4303 shows a very slight concavity. The lateral face (Fig. 6A₄) shows the flattened articular surface for the fibula and an elliptic depression below it, placed at a centrodistal position. All these features coincide with leontiniids such as *Scarrittia* (e.g., AMNH 29582, *S. canquelensis* from Sierra Canquel, Chubut Province; see also Shockey et al. 2012) and *Leontinia* (e.g., MACN A 12311, *L. gaudryi* from La Flecha,

Table 5. Measurements (in mm) of the navicular of *Gualta cuyana* from Quebrada Fiera, Mendoza, compared with that of *Scarrittia canquelensis* from Chubut Province. Photographs of *Scarrittia* taken by Barbara Vera and Andrea Elissamburu. Values in parentheses are approximate. APD, anteroposterior diameter; H, height; TD, transversal diameter; – measurement not available.

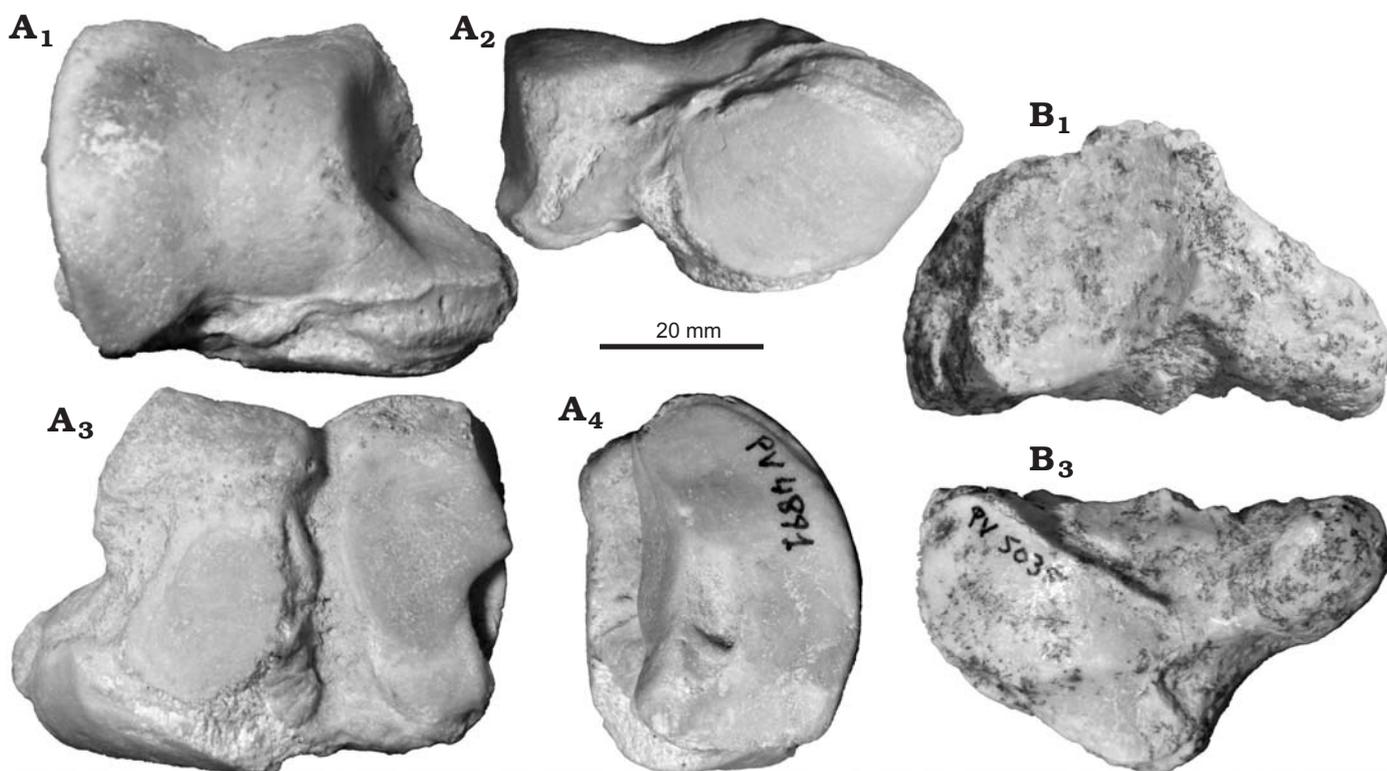| Navicular	Maximum TD	Proximal articulation TD	Maximum APD	Corpus maximum H	Apophysis H
Gualta cuyana MCNAM-PV 5035	32.0	25.2	53.5	19.9	17.7
Scarrittia canquelensis AMNH 29585	51.6	40.6	83.7	–	(22.5)

Fig. 6. Tarsal bones of leontiniid notoungulate *Gualta cuyana* Cerdeño and Vera, 2015 from Quebrada Fiera, Mendoza, Argentina; Deseadan SALMA (late Oligocene). **A**. MCNAM-PV 4891, right astragalus, anterior (A₁), distal (A₂), posterior (A₃), and lateral (A₄) views. **B**. MCNAM-PV 5035, left navicular, anterior face to the left, proximal (B₁) and distal (B₂) views.

Santa Cruz Province), in which the trochlea is even a little deeper than in the studied astragali. In contrast, the compared astragali of early Miocene toxodontids differ in the deeper trochlea, the distal area a little more detached, the medial facet for the calcaneum wider distally and the lateral depression centroproximally placed.

The navicular MCNAM-PV 5035 (Fig. 6B, Table 5) is composed of a main corpus with the articular facets and a long, narrow and curved posterolateral apophysis, resulting in a relatively narrow and deep (APD) bone. The proximal face (Fig. 6B₁) is occupied by a large anteroposteriorly concave facet for the astragalus; its outline is rather square, but two small portions project posteriorly, leaving a wide notch in between. At the level of this notch, the apophysis develops and is directed posteriorly and laterally. In distal view (Fig. 6B₂), there are two main facets, a medial one for the mesocuneiform and a larger, lateral one for the ectocuneiform; the former is convex-concave whereas the latter is smoothly convex anteroposteriorly; both facets are placed in a continuous surface with a crest in between. There is no articulation for the entocuneiform. Also seen in distal view, there is a small lateral facet for the cuboid, which in turn forms an acute angle with another lateral facet for the calcaneum. In lateral view, the apophysis surpasses a little the distal face. The anterior and medial faces form a continuous rugose surface, without forming great tuberosities. This morphology coincides with that of *Scarrittia canquelensis* (Chaffee 1952) and differs from toxodontids in the

presence of a large posterior apophysis. Similarities are evident when comparing MCNAM-PV 5035 with the photographs of the homologous bone of the specimen AMNH 29585, but the size of the latter is much greater. According to our estimates for AMNH 29585, the navicular of *G. cuyana* is around 36–38% smaller than that of *S. canquelensis* (Table 5).

Concerning notohippid morphology, the astragalus of this group is closer to the homologous bone in the toxodontid *Proadinotherium* (see comments above) than to the specimens assigned to *Gualta*.

Remarks.—Within the Quebrada Fiera fauna, the leontiniid *Gualta cuyana* was described based on a skull and associated vertebrae, and some mandibular fragments, but some limb elements (calcanei and humeri) were also originally assigned to this taxon (Cerdeño and Vera 2015). The present study has allowed the reinterpretation, both anatomically and taxonomically, of some postcranial bones preliminarily identified as toxodontids (Hernández Del Pino et al. 2013), which are described and discussed below.

Stratigraphic and geographic range.—Late Oligocene; Mendoza Province, Argentina.

Homalodotheriidae Huxley, 1870

Genus *Asmodeus* Ameghino, 1894

Type species: *Asmodeus osborni* Ameghino, 1894, La Flecha?, Santa Cruz Province, Argentina, Deseadan SALMA, late Oligocene.
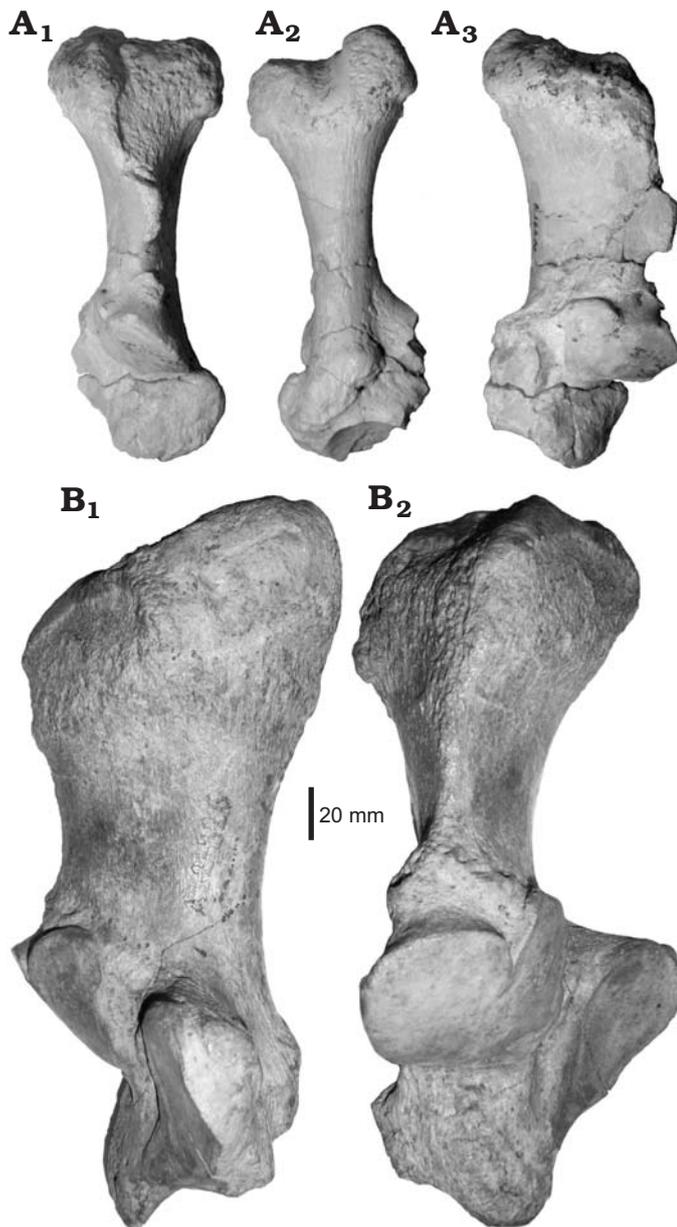
Fig. 7. Homalodotheriid notoungulate *Asmodeus* from Argentina. **A**. *Asmodeus petrasnerus* Seoane and Cerdeño, 2014, from Quebrada Fiera, Mendoza; Deseadan SALMA (late Oligocene), MCNAM-PV 4958, left calcaneum, anterior (A$_1$), posterior (A$_2$) and medial (A$_3$) views. **B**. *Asmodeus osborni* Ameghino, 1894 from Santa Cruz; Deseadan SALMA (late Oligocene), MACN A 12327, holotype, right calcaneum, medial (B$_1$) and anterior (B$_2$) views.

Asmodeus petrasnerus Seoane and Cerdeño, 2014

Fig. 7A.

Material.—MCNAM-PV 4958, left calcaneum; MCNAM-PV 5077, fragment of left calcaneum from Quebrada Fiera, Mendoza, Argentina, Deseadan SALMA, late Oligocene.

Emended diagnosis.—The calcaneum MCNAM-PV 4958 allows establishing new characteristics for *A. petrasnerus*, which is reflected in the following emended diagnosis. Calcaneum with well-developed tendinous sulcus in the

tuber and anterior border of the neck projected and with a distal semicircular notch, both features differing from *Asmodeus osborni* and *Homalodotherium*; mediodistal facet for the navicular as in *A. osborni* but subtriangular in outline; ectal facet with concave medial border as in *A. osborni* and differing from *Homalodotherium*; anterodistal end and distal facet little projected in contrast with *A. osborni* and *Homalodotherium*; astragalus with articular head very convex and more medially placed than in *A. osborni*, separated by a wider neck from the corpus; astragalar groove expanded as in *A. osborni*; absence of astragalar foramen as in *Homalodotherium*; cuboid relatively wider than in *Homalodotherium* and without contact with the astragalus; Mc III with proximal facet more extended posteriorly than in *Homalodotherium*, crescent-shaped and at an acute angle with lateral facets; Mc IV with the groove between medial facets extended to the proximal edge in contrast with *Homalodotherium*.

Description.—The specimen MCNAM-PV 4958 (Fig. 7A; Table 1) is a large and robust left calcaneum; it is almost complete, only the sustentacular facet is broken at its medial region. The tuber is massive (Fig. 7A$_1$), subtriangular in outline, with a rounded lateral vertex. A well-developed tendinous sulcus crosses from the most posterior border to the anterior apex, separating a lateral and a smaller medial calcaneal processes, the latter more projected proximally (Fig. 7A$_2$). The neck is long and narrow, and its anterior

Table 6. Results from the extended implied weighting analysis under different values of k (concavity constant). "Steps" indicate the number of steps of MPTs obtained, "Trees" indicate the number of MPTs obtained, "Fit" indicates the fit value for the MPTs and "Sprdif" indicates the subtree pruning regrafting distances between successive k values used in the analysis.

k	Steps	Trees	Fit	Sprdif
0.680412	166	10	25.183075	0
0.737113	166	10	24.56714	0
0.798745	166	10	23.935236	0
0.865979	166	10	23.286482	0
0.939617	166	10	22.619878	0
1.020618	166	10	21.934355	0
1.110146	166	10	21.228703	0
1.209621	166	10	20.5016	0
1.3208	166	10	19.751546	0
1.445876	166	10	18.976887	0
1.587628	166	10	18.175743	0
1.749631	166	10	17.345976	0
1.936557	166	10	16.485162	0
2.154638	166	10	15.590503	0
2.41237	166	10	14.658772	0
2.721648	166	10	13.686199	0
3.099655	164	50	12.661803	1
3.572163	164	50	11.57131	0
4.179674	164	50	10.42628	0
4.989688	164	50	9.21974	0
6.123708	164	50	7.943128	0

border forms a thin projection between the tuber and the fibular facet, showing a marked semicircular notch at its distal end (Fig. 7A₃); this notch could surround a soft structure that, judging by the size, could be a tendon or ligament. The articular area is short and coincides with the holotype of *A. petrasnerus* (MCNAM-PV 4101; Seoane and Cerdeño 2014); the posterior tuberosity or plantar tubercle (better seen in posterior view; Fig. 7A₂) is similar to that of the holotype, but is less projected distally than in the specimen MCNAM-PV 3906 (included, but not figured by Seoane and Cerdeño 2014); this difference is interpreted as intraspecific variation. The morphology of MCNAM-PV 4958 differs from both *A. osborni* (e.g., MACN A 12327, Fig. 7B; AMNH 11735) and *Homalodotherium* (e.g., MACN A 8611, AMNH 9261) in the more developed tendinous sulcus and the projected anterior border with a distal notch, which add to the diagnostic characters of *A. petrasnerus*. The size of MCNAM-PV 4958 is clearly smaller than that of *A. osborni* (Table 1, Fig. 7B); this difference in size was not mentioned by Seoane and Cerdeño (2014: fig. 5) and was not reflected in the corresponding figure due to a scale mistake.

Besides MCNAM-PV 4958, a fragment of a left calcaneum, MCNAM-PV 5077, was also recovered. It only preserves the distal part of the sustentacular facet and most of the ectal and fibular facets, which do not differ from the previous specimens of *A. petrasnerus*; the slightly greater size of the facets reflects a larger individual.

Stratigraphic and geographic range.—Late Oligocene; Mendoza Province, Argentina.

Phylogenetic analysis

The traditional search for equally weighted characters resulted in 408 trees of 163 steps (Consistency Index: 0.595, Retention Index: 0.773), whose strict consensus tree is presented in Fig. 8A. The consensus tree has a basal unresolved polytomy of six taxa: *Asmodeus osborni, A. petrasnerus, Homalodotherium cunninghami, Thomashuxleya externa, Anisotemnus distentus* and the clade comprising Leontiniidae, "Notohippidae", and Toxodontidae. The internal relationships of "Notohippidae" and Leontiniidae remain mostly unresolved. *Eurygenium* appears in a trichotomy with two major clades, one comprising the rest of the notohippids and toxodontids and the other gathering the leontiniids. That is, "notohippids" result paraphyletic as in previous analyses whereas toxodontids and leontiniids form monophyletic groups, but with very low support for the latter (GC "jack-knife" node support = 16).

The reduced consensus analysis (see Material and methods and SOM 3) provided a tree with a total of 19 terminal taxa and 6 pruned taxa: *Martinmiguelia fernandezi, Taubatherium paulacoutoi, Ancylocoelus frequens, Huilatherium pluriplicatum, Asmodeus petrasnerus*, and the *Colpodon* clade (Fig. 8B). In this consensus, the position of *A. petrasnerus* floats from the basal polytomy of the tree to a polytomy with *A. osborni* and *Homalodotherium cunninghami* (recovering, in this case, the Homalodotheriidae) and to a final arrangement as sister taxon of *A. osborni*. Also, this analysis shows alternative positions within the leon-
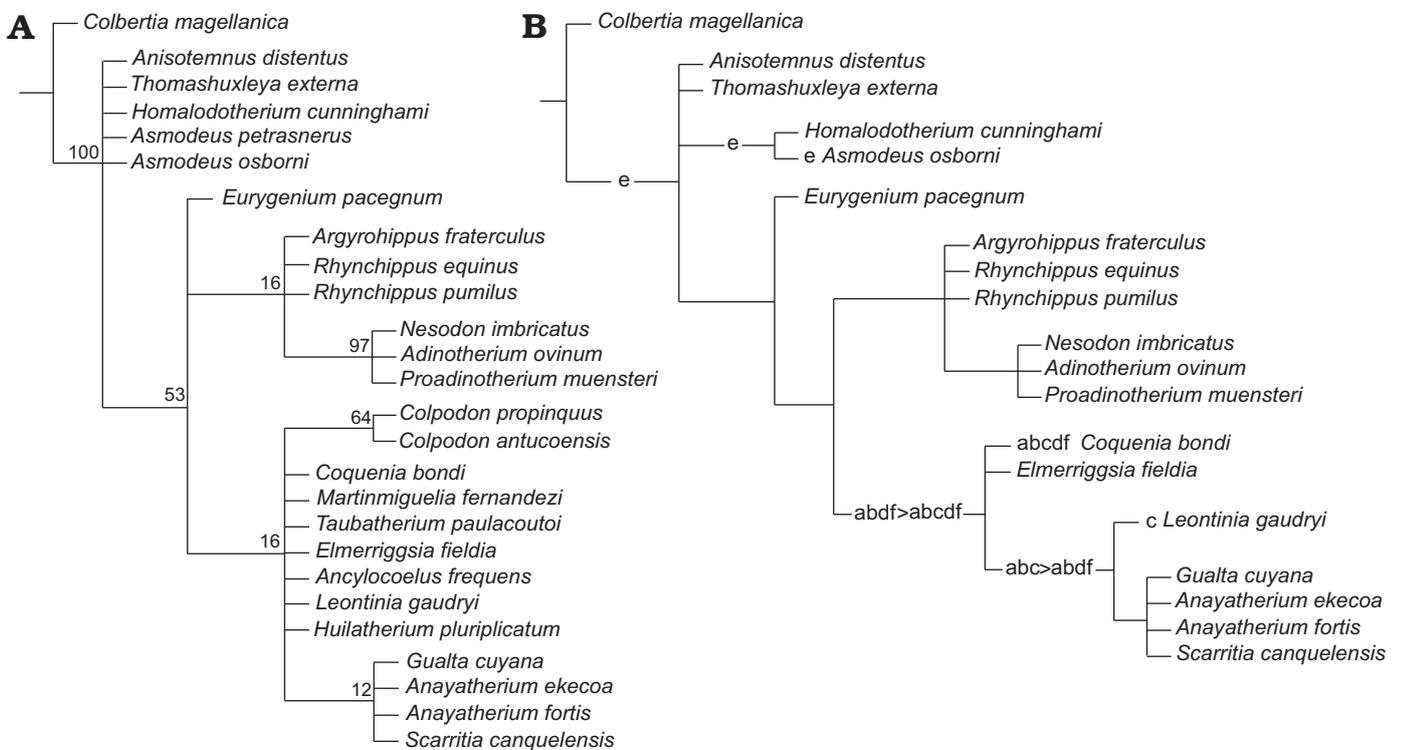

Fig. 8. Consensus trees from phylogenetic analyses under equal weights. **A**. Strict consensus tree. **B**. Reduced consensus tree. a, *Martinmiguelia fernandezi*; b, *Taubatherium paulacoutoi*; c, *Ancylocoelus frequens*; d, *Huilatherium pluriplicatum*; e, *Asmodeus petrasnerus*; f, *Colpodon antucoensis + C. propinquus*.
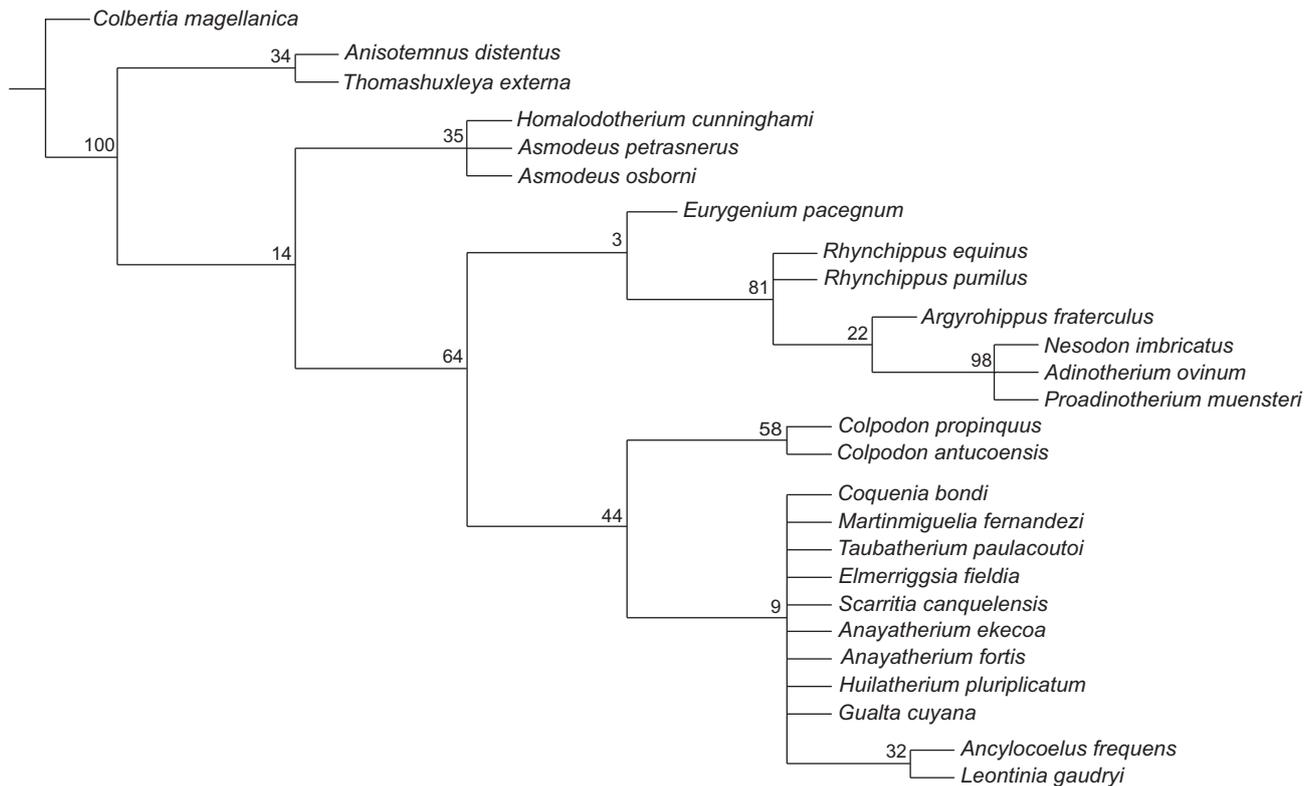
Fig. 9. Strict consensus tree from phylogenetic analysis under extended implied weighting with 21 different values of k.

tiniid clade for *M. fernandezi*, *T. paulacoutoi*, *An. frequens*, *H. pluriplicatum*, and the clade with the two species of *Colpodon*, *An. frequens* being the only taxon with an alternative position related to *Leontinia*. The decision to present this alternative is to provide a more informative and complementary arrangement to the strict consensus under equal weights. In addition, we provide a list of the evaluated characters involved in the alternative positions of the unstable taxa (see SOM 3).

Results of the analysis using extended implied weights under different values of k are summarized in Table 6 (see also SOM 4 for other results from this analysis). When running the analyses with various k values under 2.72, the number of trees stabilizes at 10 and tree topology of the strict consensus for each k value remains unchanged (SOM 4: fig. 4). With k values above 2.72 (3.10–6.12), the analysis results in 50 trees for each value and the strict consensus presents the same topology (SOM 4: fig. 4). The use of weighting against homoplasy under all values of k evaluated (0.68–6.12) provided a consensus tree (Fig. 9) better resolved than under equal weights. The major differences are: (i) recovery of the Homalodotheriidae clade; (ii) better resolution for "notohippid" relationships; (iii) *Argyrohippus* as sister taxon of the Toxodontidae; (iv) the *Colpodon* clade as sister taxon of the remaining Leontiniidae; and (v) *Leontinia* gathered in a clade with *Ancylocoelus*. We present this tree topology for comparative purposes only, instead of using one particular value because we lack a clear criterion for selecting proper values of k.

It is important to note that, according to Goloboff (1993), the decision of which value of k to use probably depends on the dataset. The lower the k values are, the greater the penalty that homoplasy receives (Goloboff 1993). Given the fact that the taxon sampling of this matrix does not represent the entire diversity within Toxodontia, estimation of homoplasy in characters may be affected, because the species in which these traits vary homoplastically are absent (Juan M. Mirande personal communication, April 2016). Therefore, the use of high penalizations against homoplasy might be inadvisable even when the TNT routine used here suggests otherwise.

Exclusive and non-exclusive synapomorphies for the strict consensus trees under equal and implied weights are detailed in SOM 4. The considered postcranial features provide some resolution at the basal nodes of the trees, but the results can be biased by the lack of knowledge of postcranium in many compared species.

Conclusions

The study of different postcranial bones, particularly carpals and tarsals, from Quebrada Fiera provides new anatomical data for several Deseadan notoungulates of the suborder Toxodontia.

On the one hand, toxodontids from this locality are herein described for the first time, and a few teeth are also included in the study. We recognize two taxa, *Proadinotherium* sp.

and Toxodontidae gen. et sp. indet. The three teeth, astragalus and calcaneum assigned to *Proadinotherium* sp. represent the first mention of this genus in Argentina outside Patagonia, and add to the other extra-Patagonian record (*P. saltoni*) from Salla, Bolivia. The recognition of a second toxodontid is based on a fragment of calcaneum that precludes a precise taxonomic determination; it might correspond to the other Deseadan genus, *Pronesodon*, a taxon that has not been so far recorded outside Patagonia, and whose systematic revision is pending.

On the other hand, several foot bones preliminarily considered to belong to toxodontids are now recognized as leontiniids and assigned to *Gualta cuyana*, increasing the knowledge of the postcranial anatomy of this endemic species.

Similarly, the finding of a complete calcaneum of a homalodotheriid has revealed new data for *Asmodeus petrasnerus*, allowing the addition of two new diagnostic characters.

The use of various phylogenetic approaches to analyze the data and the new material included in this study allowed us to provide a more robust set of information, even though the final tree topologies do not differ much from those previously published. Mapping synapomorphies for the resulting trees shows that postcranial features provide resolution at the basal nodes of the trees whereas dental features do that at the terminals.

Acknowledgements

References

Ameghino, F. 1887. Enumeración sistemática de las especies de mamíferos fósiles coleccionados por Carlos Ameghino en los terrenos eocenos de Patagonia austral y depositados en el Museo de La Plata. *Boletín del Museo de La Plata* 1: 1–26.

Ameghino, F. 1889. *Trachytherus spegazzinianus, nuevo mamífero fósil del orden de los toxodontes*. 8 pp. P.E. Coni, Buenos Aires.

Ameghino, F. 1891. Nuevos restos de mamíferos fósiles descubiertos por Carlos Ameghino en el Eoceno inferior de Patagonia austral. Especies nuevas: adiciones y correcciones. *Revista Argentina de Historia Natural* 1: 289–328.

Ameghino, F. 1894. Première contribution à la conaissance de la faune mammalogique des couches à *Pyrotherium*. *Boletín del Instituto Geográfico Argentino* 15: 603–660.

Ameghino, F. 1897. Mamíferos cretáceos de la Argentina. Segunda contribución al conocimiento de la fauna mastológica de las capas con restos de *Pyrotherium*. *Boletín Instituto Geográfico Argentino* 18: 406–521.

Ameghino, F. 1902. Première contribution à la connaissance de la fauna mammalogique des couches à *Colpodon*. *Boletín de la Academia Nacional de Ciencias de Córdoba* 17: 71–141.

Berqvist, L.P. and Ribeiro, A.M. 1998. A paleomastofauna das bacias eoterciárias brasileiras e sua importância na dataçao das bacias de Itaboraí e Taubaté. *Asociación Paleontológica Argentina, Publicación especial* 5: 19–34.

Billet, G. 2011. Phylogeny of the Notoungulata (Mammalia) based on cranial and dental characters. *Journal of Systematic Paleontology* 9: 481–497.

Bond, M. 1986. Los ungulados fósiles de Argentina: evolución y paleoambientes. *IV Congreso Argentino de Paleontología y Bioestratigrafía, Mendoza, Actas* 2: 173–185.

Bond, M. and López, G. 1995. Los mamíferos de la Formación Casa Grande (Eoceno) de la provincia de Jujuy, Argentina. *Ameghiniana* 32: 301–309.

Cassini, G.H., Cerdeño, E., Villafañe, A.L., and Muñoz, N.A. 2012. Paleobiology of Santacrucian native ungulates (Meridiungulata: Astrapotheria, Litopterna and Notoungulata. *In*: S.F. Vizcaíno, R. Kay, and M.S. Bargo (eds.), *Early Miocene Paleobiology in Patagonia: High-Latitude Paleocommunities of the Santa Cruz Formation*. 370 pp. Cambridge University Press, Cambridge.

Cerdeño, E. 2014. First record of Mesotheriidae in the late Oligocene of Mendoza Province, Argentina. *Ameghiniana* 51: 366–370.

Cerdeño, E. and Vera, B. 2010. *Mendozahippus fierensis*, gen. et sp. nov., new Notohippidae (Notoungulate) from the late Oligocene of Mendoza (Argentina). *Journal of Vertebrate Paleontology* 30: 1805–1817.

Cerdeño, E. and Vera, B. 2014. New data on diversity of Notohippidae from the Oligocene of Mendoza, Argentina. *Journal of Vertebrate Paleontology* 34: 941–950.

Cerdeño, E. and Vera, B. 2015. A new Leontiniidae (Notoungulata) from the late Oligocene beds of Mendoza Province, Argentina. *Journal of Systematic Paleontology* 13: 943–962.

Cerdeño, E., Vera, B., Schmidt, G. I., Pujos, F., and Mamaní Quispe, B. 2012. An almost complete skeleton of a new Mesotheriidae (Notoungulata) from the Late Miocene of Casira, Bolivia. *Journal of Systematic Paleontology* 10: 341–360.

Chaffee, R.G. 1952. The Deseadan vertebrate fauna of the Scarritt Pocket, Patagonia. *Bulletin of the American Museum of Natural History* 98: 503–562.

Cifelli, R.L. 1983. Eutherian tarsals from the Late Paleocene of Brazil. *American Museum Novitates* 2761: 1–31.

Cifelli, R.L. 1993. The phylogeny of the native South American ungulates. *In*: F.S. Szalay, M.J. Novacek, and M.C. McKenna (eds.), *Mammals Phylogeny: Placentals*. 601 pp. Springer-Verlag, New York.

Combina, A.M. and Nullo, F. 2011. Ciclos tectónicos, volcánicos y sedimentarios del Cenozoico del sur de Mendoza-Argentina (35°–37°S y 69°30'W). *Andean Geology* 38: 198–218.

Constantinescu, G.M. and Schaller, O. 2012. *Illustrated Veterinary Anatomical Nomenclature. 3rd Edition*. 614 pp. Ferdinand Enke Verlag, Stuttgart.

Croft, D.A. 1999. Placentals: endemic South American ungulates. *In*: R. Singer (ed.), *The Encyclopedia of Paleontology*. 1550 pp. Fitzroy-Dearborn, Chicago.

Deraco, M.V. and García López, D. 2015. A new Eocene Toxodontia (Mammalia, Notoungulata) from northwestern Argentina. *Journal of Vertebrate Paleontology* 36: e1037884.

Deraco, M.V, Powell, J.E., and López, G. 2008. Primer leontínido (Mammalia, Notoungulata) de la Formación Lumbrera (Subgrupo Santa Bár-

bara, Grupo Salta-Paleógeno) del noroeste Argentino. *Ameghiniana* 45: 83–91.

Elissamburu, A. 2010. Estudio biomecánico y morfofuncional del esqueleto apendicular de *Homalodotherium* Flower 1873 (Mammalia, Notoungulata). *Ameghiniana* 47: 25–43.

Flower, W.H. 1873. On a newly discovered extinct ungulate mammal from Patagonia, *Homalodontotherium cunninghami*. *Philosophical Transactions of the Royal Society of London* 164: 173–182.

Forasiepi, A.M., Cerdeño, E., Bond, M., Schmidt, G.I., Naipauer, M., Straehl, F.R., Martinelli, A.G., Garrido, A.C., Schmitz, M.D., and Crowley, J.L. 2015. New toxodontid (Notoungulata) from the Early Miocene of Mendoza, Argentina. *Paläontologische Zeitschrift* 89: 635–643.

Forasiepi, A.M., Goin, F.J., Abello, M.A., and Cerdeño, E. 2014. A unique, Late Oligocene shrew-like marsupial from western Argentina and the evolution of dental morphology. *Journal of Systematic Palaeontology* 12: 549–564.

Goloboff, P. 1993. Estimating character weights during tree search. *Cladistics* 9: 83–91.

Goloboff, P. 2014. Extended implied weighting. *Cladistics* 30: 260–272.

Goloboff, P., Farris, S., and Nixon, K. 2008. TNT, a free program for phylogenetic analysis. *Cladistics* 24: 774–786.

Gorroño, R., Pascual, R., and Pombo, R. 1979. Hallazgo de mamíferos eógenos en el sur de Mendoza. Su implicancia en las dataciones de los "rodados lustrosos" y del primer episodio orogénico del Terciario en esa región. *VII Congreso Geológico Argentino, Actas*: 475–487, Asociación Geológica Argentina, Neuquén.

Hernández Del Pino, S., Seoane, F., and Cerdeño, E. 2013. Toxodontidae y Homalodotheriidae del Oligoceno tardío de Quebrada Fiera, Mendoza, centro-oeste de Argentina. *VIII Congreso Latinoamericano de Paleontología y XIII Congreso Mexicano de Paleontología*, *Programa y Resúmenes*: 56, Guanajuato.

Huxley, T.H. 1870. Anniversary Address of the President. *Quarterly Journal Geological Society of London* 26: xxix–lxiv.

Lorente, M., Gelfo, J.N., and López, G.M. 2014. Postcranial anatomy of the early notoungulate *Allalmeia atalaensis* from the Eocene of Argentina. *Alcheringa* 38: 398–411.

Madden, R. 1990. *Miocene Toxodontidae (Notoungulata, Mammalia) from Colombia, Ecuador and Chile*. 406 pp. Unpublished Ph.D. Dissertation, Duke University, North Carolina.

Miquel, S.E. and Cerdeño, E. 2016. First record of the Chilean gastropod *Chiliborus* in the Oligocene of Mendoza (Argentina) (Gastropoda Pulmonata: Strophocheilidae). *Archiv für Molluskenkunde* 145: 1–6.

Mirande, J.M. 2009. Weighted parsimony phylogeny of the family Characidae (Teleostei: Characiformes). *Cladistics* 25: 574–613.

Mirande, J.M., Camargo Jerep, F., and Vanegas-Ríos, J.A. 2013. Phylogenetic relationships of the enigmatic *Carlastyanax aurocaudatus* (Eigenmann) with remarks on the phylogeny of the Stevardiinae (Teleostei: Characidae). *Neotropical Ichthyology* 11: 747–766.

Nassif, N.L., Musalem, S., and Cerdeño, E. 2000. A new toxodont from the Late Miocene of Catamarca, Argentina, and a phylogenetic analysis of the Toxodontidae. *Journal of Vertebrate Paleontology* 20: 591–600.

Nixon, K.C. 2002. *WinClada ver. 1.00.08*. Published by the author, Ithaca.

Owen, R. 1845. *Descriptive and Illustrated Catalogue of the Fossil Organic Remains of Mammalia and Aves Contained in the Museum of the Royal College of Surgeons of England*. 391 pp. R. and J.E. Taylor, London.

Owen, R. 1853. Description of some species of the extinct genus *Nesodon*, with remarks on the primary group (Toxodontia) of hoofed quadrupeds, to which that genus is referable. *Philosophical Transactions of the Royal Society of London* 143: 291–310.

Patterson, B. and Pascual, R. 1972. The fossil mammal fauna of South America. *In*: A. Keast, F.C. Erk, and B. Glass (eds.), *Evolution, Mammals, and Southern Continents*. 543 pp. University of New York State Press, Albany.

Pol, D. and Escapa, I.H. 2009. Unstable taxa in cladistic analysis: identification and the assessment of relevant characters. *Cladistics* 25: 515–527.

Ribeiro, A.M. and Bond, M. 2000. New data about the Notoungulata (Leontiniidae and Notohippidae) from Tertiary of Acre State, Brazil. *Geociências* 5: 47–53.

Roth, S. 1903. Los ungulados sudamericanos. *Anales del Museo de La Plata, Paleontología* 5: 5–36.

Scott, W.B. 1912. Palaeontology. II, Toxodonta of the Santa Cruz beds; III, Entelonychia of the Santa Cruz beds. *Reports of the Princeton University Expeditions to Patagonia 1896–1899* 6: 111–238.

Seoane, F. and Cerdeño, E. 2014. First extra-Patagonian record of *Asmodeus* Ameghino (Notoungulata, Homalodotheriidae) in the Late Oligocene of Mendoza Province, Argentina. *Ameghiniana* 51: 373–384.

Shockey, B.J. 1997. Two new notoungulates (Family Notohippidae) from the Salla Beds of Bolivia (Deseadan: Late Oligocene): systematics and functional morphology. *Journal of Vertebrate Paleontology* 17: 584–599.

Shockey, B.J. and Anaya, F. 2008. Postcranial osteology of mammals from Salla, Bolivia (Late Oligocene): form, function, and phylogenetic implications. *In*: E.J. Sargis and M. Dagosto, (eds.), *Mammalian Evolutionary Morphology: a Tribute to Frederick S. Szalay*. 439 pp. Springer, Dordrecht.

Shockey, B.J., Billet, G., and Salas Gismondi, R. 2016. A new species of *Trachytherus* (Notoungulata: Mesotheriidae) from the late Oligocene (Deseadan) of Southern Peru and the middle latitude diversification of early diverging mesotheriids. *Zootaxa* 4111: 565–583.

Shockey, B.J., Croft, D. A., and Anaya, F. 2007. Analysis of function in the absence of extant functional homologues: a case study using mesotheriid notoungulates. *Paleobiology* 33: 227–247.

Shockey, B.J., Flynn, J.J., Croft, D.A., Gans, P.B., and Wyss, A.R. 2012. New leontiniid Notoungulata (Mammalia) from Chile and Argentina: comparative anatomy, character analysis, and phylogenetic hypotheses. *American Museum Novitates* 3737: 1–64.

Simpson, G.G. 1934. A new notoungulate from the early Tertiary of Patagonia. *American Museum Novitates* 735: 1–3.

Simpson, G.G. 1936. Structure of a primitive Notoungulate cranium. *American Museum Novitates* 824: 1–31.

Simpson, G.G. 1945. The principles of classification and a classification of mammals. *Bulletin of the American Museum of Natural History* 85: 1–350.

Villarroel, C. and Colwell Danis, J. 1997. A new leontiniid notoungulate. *In*: R.F. Kay, R.H. Madden, R.L. Cifelli, and J.J. Flynn (eds.), *Vertebrate Paleontology in the Neotropics. The Miocene Fauna of La Venta, Colombia*. 608 pp. Smithsonian Institution Press, Washington DC.